

Study of the ballistic behaviour of UHMWPE composite material: experimental characterization and numerical simulation

Hakim Abdulhamid^{1, *}, Paul Deconinck¹, Pierre-Louis Héreil¹ and Jérôme Mespoulet¹

¹Thiot Ingénierie, Route Nationale, 46130 Puybrun, France

1 Abstract

This paper presents a comprehensive mechanical study of UHMWPE (Ultra High Molecular Weight Polyethylene) composite material under dynamic loadings. The aim of the study is to provide reliable experimental data for building and validation of the composite material model under impact. Three types of dynamic characterization tests have been conducted: in-plane tension, out-of-plane compression and out-of-plane shear. Moreover, impacts of spherical projectiles impact have been performed on larger specimen. Regarding the numerical simulation, an intermediate scale multi-layered model (between meso and macro scale levels) is proposed. The material response is modelled with a 3d elasto-orthotropic law coupled with fiber damage model. The modelling choice using *MAT_ORTHOTROPIC_SIMPLIFIED_DAMAGE is governed by a balance between reliability and computational cost. Material dynamic response is unconventional [1, 2]: it shows large deformation before failure and very low shear modulus and peeling strength. Numerical simulation has been used both during the design and the analysis of tests. Mechanical properties related to elastic moduli and failure strength have been measured. The ballistic numerical model is able to reproduce the main behaviors observed in the experiment. The study has highlighted the influence of temperature and fiber slipping in the impact response of the material.

2 Introduction

The use of polymer-based composite like polypropylene, aramid and ultra-high molecular weight polyethylene (UHMWPE) has become more and more popular in lightweight armours. Due to their composite structure, such type of material can exhibit diverse failure modes depending on the characteristics (geometry, material, velocity) of the impactor. Therefore, it becomes convenient to use numerical tool for the analysis and optimisation of such type of armour against different threats. Many studies have been conducted on UHMWPE composite material dynamic response. For example, [1] investigated in-plane deformation behaviour and [2] shock propagation in-fibre direction. Out-of-plane compressive response has been studied under static [3] and [4] shock loading. Furthermore, a comprehensive literature is available regarding, the ballistic response of such material [5-6]. [6] used a numerical model combining orthotropic behaviour and EOS for the simulation of ballistic response on UHMWPE plate.

This paper describes a study combining experimental and numerical tools to develop a ballistic FE model for UHMWPE composite panel. The material mechanical response and failure mode are investigated under four types of dynamic solicitation: in-plane tension, out-of-plane compression and out-of-plane shear. Then, ballistic impact tests are performed with spherical projectile. Experimental data is then used as input of an orthotropic material law coupled with fibre damage. The paper is divided into two main parts, the first section details the characterisation tests and the second section deals with the ballistic tests and simulation. Results are normalized to comply with the confidentiality obligations of the study.

3 Material characterisation

The material is available as a stratified composite panel of UHMWPE unidirectional fibres. It is the strongest fibre available in terms of strength to weight ratio. The panel is obtained from multiple stack 0°/90° plies impregnated with thermoplastic matrix. All the tests conducted in this study have been realised from the same batch of material.

3.1 Dynamic tension

Tensile tests are conducted on a 200 tons dynamic press with the help of specific tools presented in Figure 1 which converts the compression load into tension. Tensile loading is measured with a piezoelectric sensor which is prestressed before the beginning of the test. The machine clamping jaws relative displacement is measured with a laser displacement sensor. Specimen shape is similar to conventional tensile tests with a rectangle working area of 10 x 6 mm. The specimen is loaded at 40 s⁻¹. Tension tests are realised along the fibre direction only (0° and 90°). 45° direction tension tests could not be conducted due to a very low in-plane shearing strength of the material, the specimen fails under the clamping jaws weight.

Table 1 shows the increase in tension failure strength of the composite along the fibre direction obtained from three tests. The values have been normalized by a mean tensile strength obtained from quasi-static tests. An average 10 % increase of the strength is observed during dynamic tests.

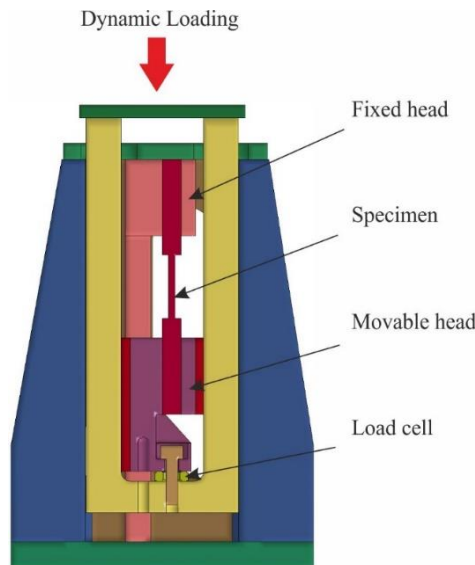


Fig. 1. Dynamic tensile tests configuration

Table 1. Normalized tensile failure strength

Test No	1	2	3	Avg.	Std. dev.
Normalized σ_{11fail} & σ_{22fail}	1.05	1.08	1.17	1.1	0.06

3.2 SHPB compression

Compression tests are conducted on Hopkinson bars. Specimens of 10x10x5 mm³ dimensions are cut with waterjet from the main plate. Compressive loading is applied in the out-of-plane (o-o-p) direction of the specimen.

Eight tests are realised with three values of striker speed to target three different mean strain rates: 3000, 4500 and 5600 s⁻¹. Figure 2 shows the evolution of the strain rate during a SHPB test. A strain rate peak is reached between 0.05 and 0.10 of deformation, then it decreases until failure. For all tests, the compressive stress versus compressive strain of the material exhibits a linear response until failure. The o-o-p compression failure mode of this composite material is quite unconventional. Failure is triggered by ply slipping near the edges of the specimen as illustrated in Figure 3-Left. Due to a very low in-plane shear strength of the material ply cannot sustain the shear stress induced by the compressive load. The slipping is initiated near the edges since the material is less confined in those areas. Similar behaviour has been reported under quasi-static loading by [3]. An increase of the failure strength is observed at high strain rate (Figure 3-Right). At 2700 s⁻¹, the failure strength increases about 20 %.

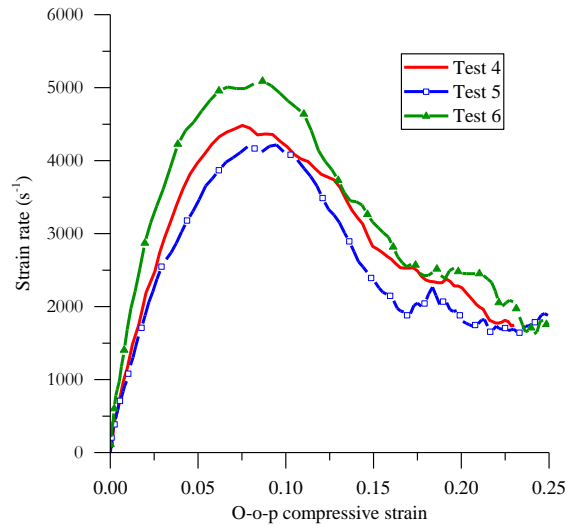


Fig. 2. Evolution of strain rate during the o-o-p compressive test

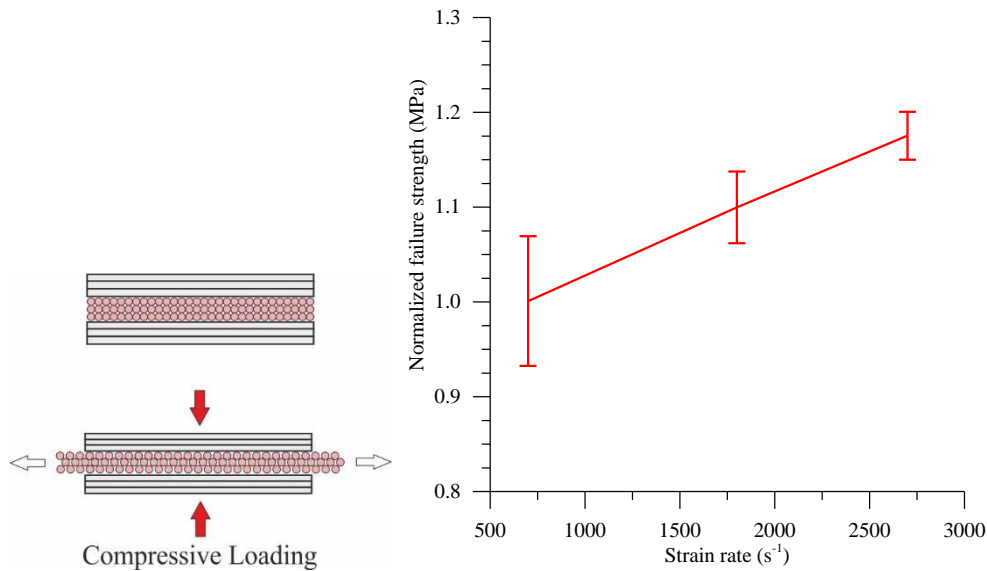


Fig. 3. Left-Failure mode under compressive o-o-p loading, Right- Strain rate effect on o-o-p compressive failure strength

3.3 Dynamic shear

A mean o-o-p shear response is measured with the configuration presented in Figure 4a. A cylindrical specimen is clamped on its edge and impacted by a cylindrical projectile. The diameter of the impactor is chosen to be slightly smaller than the inner diameter of the specimen clamp to generate shear stress in the area in between (Figure 4b).

A load cell at the back of the fitting records the loading transmitted through the shearing of the specimen. The specimen back face velocity is measured with a Photon Doppler Velocimetry (PDV) not shown in the figure. It is then integrated to compute the o-o-p displacement δ of the specimen.

The shearing angle is computed as:

$$\alpha = \text{Arctan}\left(\frac{\delta}{l}\right) \quad (1)$$

The mean shear stress is computed from the loading F recorded by the cell:

$$\tau_{mean} = \frac{F}{\pi D e} \quad (2)$$

Where D and e are respectively the inner diameter of the clamping tool and the specimen thickness.

Four tests are realized with specimen thickness varying from 3.5 to 15 mm. Figure 5 shows the normalized shear stress versus shear angle curve obtained from all tests. The strain rate profile is also similar and ranges between 4000 and 5500 s⁻¹. The material response is quite similar for all specimen thicknesses; it confirms that the flexure contribution of the loading is negligible. The response is bilinear: a moderate slope is observed up to 0.4 shear angle and then followed by a steeper slope. The first loading phase corresponds to a pure shearing of the specimen. As the displacement increases, some part of the load is transferred as a tension into the fibers which explains the increase in the slope rate.

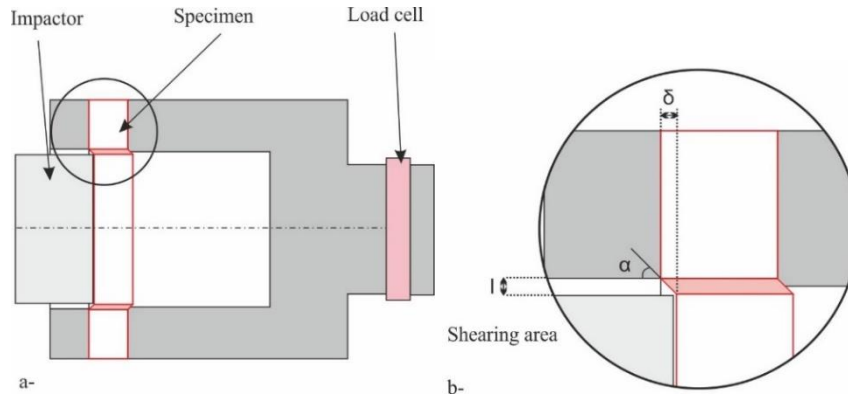


Fig. 4. Dynamic shear tests configuration

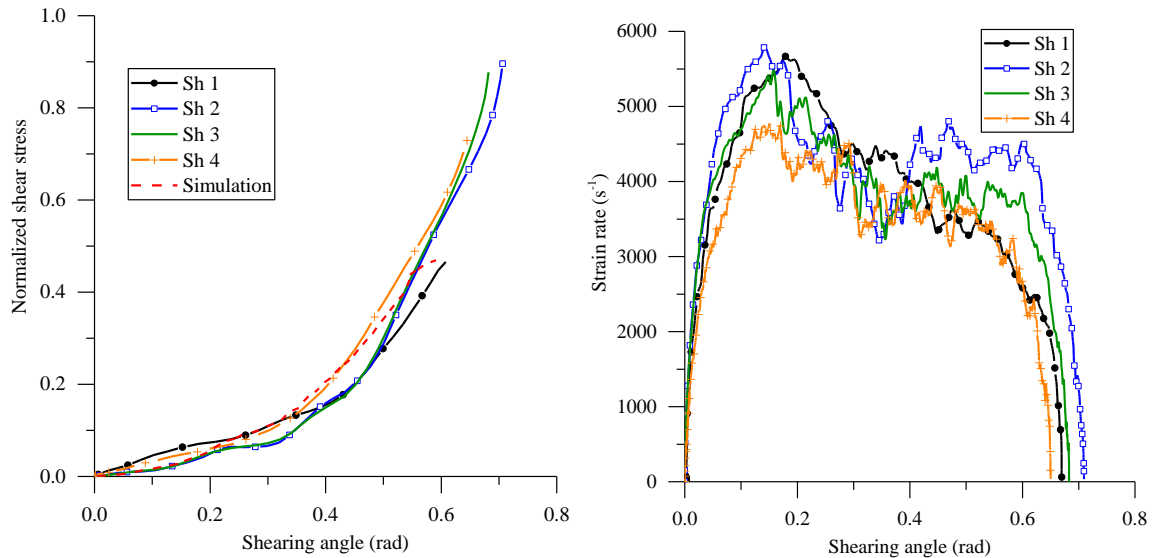


Fig. 5. Left: Normalized mean shear stress vs shearing angle, Right: Shear strain rate vs shearing angle

The identification of the shear modulus G_{13} and G_{23} can only be conducted through a reverse engineering method by simulating the test since the measured force represents an homogenized shear response all along the circumference of the specimen. The FE model is designed to replicate all the specificity of the testing condition (impactor, specimen boundary condition, load cell ...). A linear orthotropic model is used for the composite. Using an identification technique, the value of G_{13} and G_{23} is modified until the curve shear stress versus shear angle fits the experimental data (Figure 5). Figure 6 shows the localization of the shearing in the specimen in the simulation.

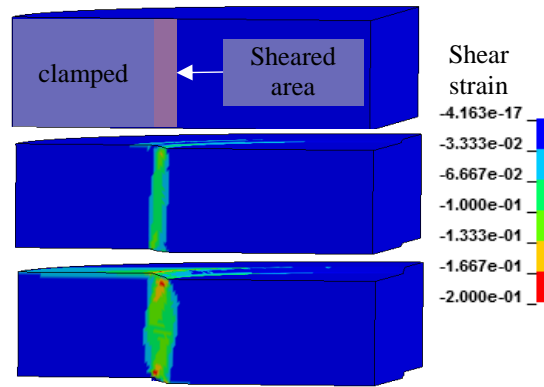


Fig. 6. Simulation of the dynamic shear test

3.4 Ballistic impact response

The study of the material is completed with ballistic impact tests. The test configuration is presented in Figure 7. A spherical steel projectile of 25 mm is launched with a gas gun. The target, a disk of 150 mm of diameter is clamped around its edge. The back face of the target is monitored with a PDV system to measure the velocity and a high-speed camera through a mirror. Two tests are performed with different target thickness in order to obtain non-perforated T11406 (Figure 8-Left) and perforated T11408 cases (Figure 8-Right).

For T11406 specimen, one third of the plies from the front side are perforated. The projectile is recovered in between plies after impact. Important ply interface delamination is observed on the perforated plies. However, the non-perforated group of plies has been compressed and densified. Around the impact point, the nature of the polymer has also changed as if it has been heated close to its melting point. The camera images show that the target undergoes an important back face deformation. Post-mortem analysis of the recovered target shows that non-failed plies undergo large slipping which explains the non-round shape of the specimen edge after the test.

For T11408 test, apart from reducing the specimen thickness, it is also conducted at a higher projectile velocity. The target is completely perforated. Its deformation is not as important as T11406 however similar signs of temperature increase is found around plies failure.

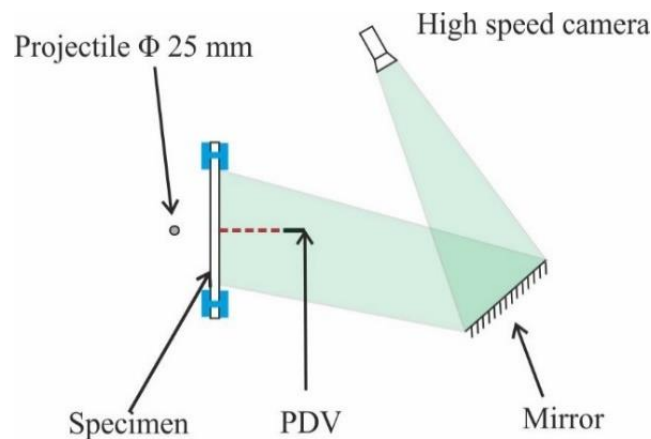


Fig. 7. Ballistic tests configuration

Considering all the information gathered throughout the characterization tests and the ballistic impact, a FE model of the ballistic test is realized in LS-DYNA (Figure 9-Left). The target is modelled in 3D at a pseudo-meso scale. Since representing each couple of 0°/90° plies by one element through the thickness would result in very large model, in the model, a set of 0°/90° is represented by one volume element.

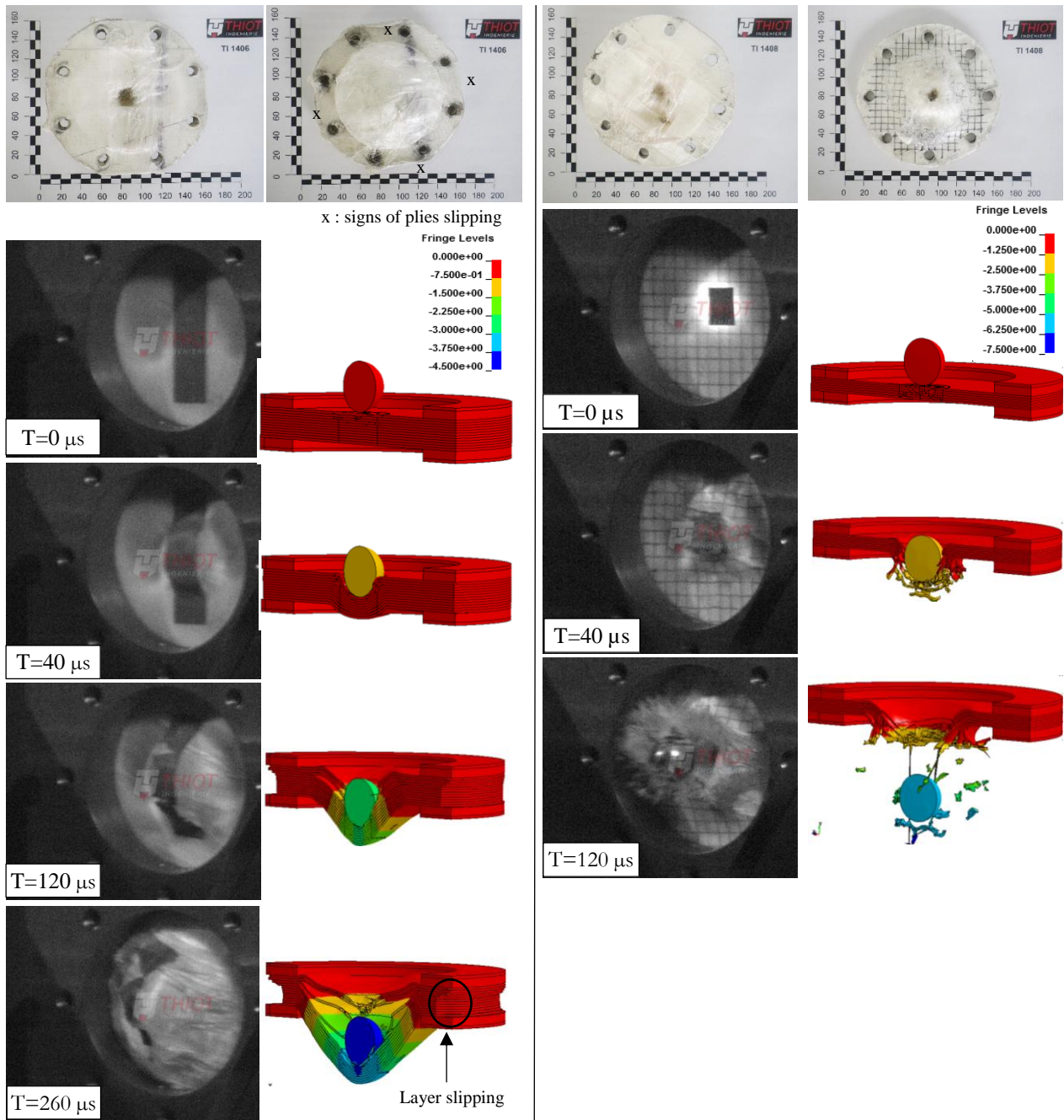


Fig. 8. Left-Non-perforated ballistic impact test (TI1406), Right-Perforated ballistic impact test (TI1408), simulations shows the o-o-p displacement in cm

Regarding the material law, initially, the orthotropic model developed in section 3.3 is used with the tensile failure strength measured in 3.1. This initial version of the model largely underestimate the ballistic limite of the material: on both cases, the projectile perforates the target with a residual velocity close to the initial projectile speed. The target does not have time to deform before it is perforated. To improve the simulation results, a damage model is added to the material model using MAT221 in LS-DYNA. The parameter for damage evolution is set to reproduce the results of TI1408. This modification is motivated to account for the softening due to temperature increase before ply failure. The comparison of obtained back face velocity and projectile residual velocity with the experimental data is shown in (Figure 9-Right). The cinematics (Figure 8-Right) of the deformation and perforation is also coherent with the test. The target is perforated before important ply slipping. This model is then used to simulate TI1406 test and results in a partially perforated target like in the test (Figure 8-Left). Furthermore, important plies slipping has occurred along the 0° and 90° as in the experiment.

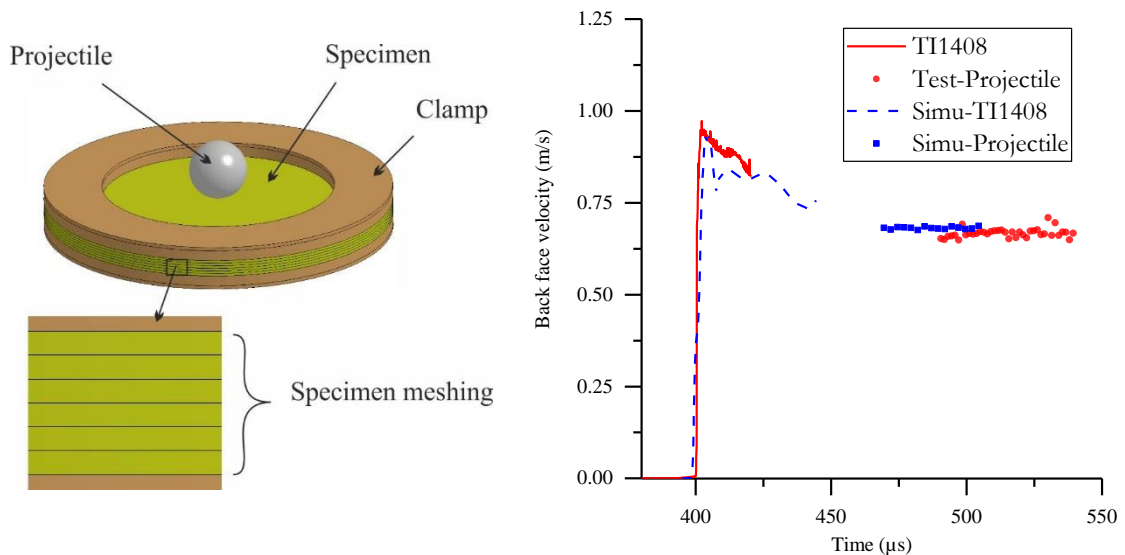


Fig. 9. Left: FE model for ballistic impact; Right: Experimental and numerical comparison of the back-face velocity of the target and projectile residual velocity for TI1408

4 Summary

In conclusion, this paper has presented a detailed characterisation study of UHMWPE composite material for shock and dynamic applications combining experimental and numerical tools. Four types of characterisation tests have been conducted: in-plane tension, out-of-plane shear, compressive responses and wave propagation. The plate mechanical response is between dry fabric and thermoplastic UD composite. UD fibre provides it with good tensile strength but the matrix low shear strength makes it prone to delamination, peeling and fibre slipping. The design and analysis of the characterisation tests have been driven by such specificity in order to acquire enough data for the building of the ballistic model. The ballistic tests have highlighted the importance of ply slipping and temperature increase in the perforation mode of the plate. The simulation approach developed in this study shows interesting results for the modelling of ballistic response of UHMWPE. The modelling scale choice represents a good compromise between calculation time and reproduction of main physical phenomena. This study should be pursued on a more detailed investigation of the failure mode of material at high temperature to confirm the modelling assumptions regarding fiber damage evolution. Another important aspect would also be the investigation of friction-dissipated energy in ply slipping.

Acknowledgments

The authors would like to thank all the team of THIOT-INGENIERIE laboratory for performing all the tests of this study.

Funding statement

This research was done with the financial support of the DGA Land Systems, French MoD.

Literature

- [1] L. Govaert, P.J. Lenstra, Colloid Polym Sci. **270** 455 (1992).
- [2] P.J. Hazell, G.J. Appleby-thomas, X. Trinquant and D.J. Chapman, J. Applied Phys., **110** (2011).
- [3] J.P. Attwood, S.N. Khaderi, K. Karthikeyan, N.A. Fleck, M.R. O'Masta, H.N.G. Wadley, V.S. Deshpande, J. Mech. Phy. Solids, **70** 200 (2014).
- [4] T. Lässig, F. Bagusat, M. May, S. Hiermaier, Int. J. Impact Eng., **86** 240 (2015).
- [5] M.R. O'Masta, B.G. Compton, E.A. Gamble, F.W. Zok, V.S. Deshpande and H.N.G. Wadley, Int. J. Imp. Eng. **86** 131 (2015).
- [6] T. Lässig, L. Nguyen, M. May, W. Riedel, U. Heisserer, H.V.D. Werff and S. Hiermaier, Int. J. Imp. Eng., **75** 110 (2015).